

## Geostatistical assessment of unconfined compressive strength of rocks in Northeast Jeddah, Saudi Arabia



Mohammed A. M. Alghamdi \*

Engineering Geology, Faculty of Earth Sciences, King Abdulaziz University, Jeddah, Saudi Arabia

### ARTICLE INFO

#### Article history:

Received 15 April 2023

Received in revised form

23 July 2023

Accepted 14 August 2023

#### Keywords:

Rock strength determination

Unconfined compressive strength

Geostatistical evaluation

Geotechnical analysis

Schmidt hammer rebound method

### ABSTRACT

The determination of rock strength holds paramount importance in the field of engineering geology. In this study, we conduct a comprehensive geostatistical evaluation of the unconfined compressive strength (UCS) within a 100 km<sup>2</sup> area situated in northeast Jeddah, Saudi Arabia. The UCS values were indirectly estimated using an empirical equation based on the Schmidt hammer rebound method, resulting in a range of strengths from 9.2 to 198.4 MPa. The corresponding mean UCS values vary between 60.3 to 81.7 MPa, with standard deviations ranging from 18.6 to 45.3 MPa. The analysis revealed that, among the sites examined, a specific location exhibited the highest median UCS value of 72.2 MPa, while another site recorded the lowest value of 56.2 MPa. Based on the distribution of UCS values, the study area was classified into five distinct strength categories: very low, low, medium, high, and very high. Notably, the majority of variability in UCS values was confined within the middle 50% range, as evident from the interquartile range (IQR) below 30 MPa. Additionally, certain sites displayed a tighter cluster of UCS values, while an IQR of  $DEF \geq 60$  indicated a more widespread distribution of strength values. Furthermore, two locations were identified as representing the minimum and maximum UCS values within a 95% confidence interval. The UCS in location A was estimated at  $60.25 \pm 9.14$  MPa, whereas in location B, it was  $81.72 \pm 8.50$  MPa. These findings offer valuable insights into the rock strength characteristics of the designated area, providing essential data for engineering and geotechnical applications.

© 2023 The Authors. Published by IASE. This is an open access article under the CC BY-NC-ND license (<http://creativecommons.org/licenses/by-nc-nd/4.0/>).

### 1. Introduction

From surface to underground mine design and construction, UCS is an essential parameter in most rock and mining engineering designs and analyses (Aladejare et al., 2021). Uniaxial compressive strength (UCS) is rocks' most frequently measured property, and it is the basis of classification in rock mechanics (González de Vallejo and Ferrer, 2011). The UCS is an index rather than a unique engineering parameter for a given rock type. Still, depending on a rock's heterogeneity, different UCS values may need to be specified for various design aspects (Bewick et al., 2015). The strength value provides information on the engineering properties of the rock. Therefore, using empirically obtained UCS from the index test would be precious for at least the preliminary

structural design stage (Yilmaz and Sendir, 2002). Uniaxial strength is the maximum that the rock can carry under uniaxial compression. It is also known as the unconfined compressive strength of the material because confining stress is set to zero (Morita, 2021). The approximate compressive strength can be estimated from correlation with indexes obtained with simple field tests, such as the Schmidt hammer test. With the values obtained, rock can be classified according to strength. Field indexes provide an initial approximation of the rock strength value.

### 2. Scope and purpose

In this case study, about 100 km<sup>2</sup> in the southern boundary of the University of Jeddah north of Jeddah city is invested (Fig. 1). The primary purpose is to classify the UCS based on Brown's (1981) criterion. The centrality, deviation, and confidence of the UCS can also be assessed using geostatistical analysis. Another goal is to produce an engineering geological map of UCS's median and interquartile range (IQR). Igneous rocks represent the constituents of the study area, but this study does not consider any

\* Corresponding Author.

Email Address: [mmushrif@kau.edu.sa](mailto:mmushrif@kau.edu.sa)

<https://doi.org/10.21833/ijaas.2023.09.011>

Corresponding author's ORCID profile:

<https://orcid.org/0000-0002-7790-5698>

2313-626X/© 2023 The Authors. Published by IASE.

This is an open access article under the CC BY-NC-ND license

(<http://creativecommons.org/licenses/by-nc-nd/4.0/>)

influencing factors such as mineral composition, texture, structural characteristics, etc.

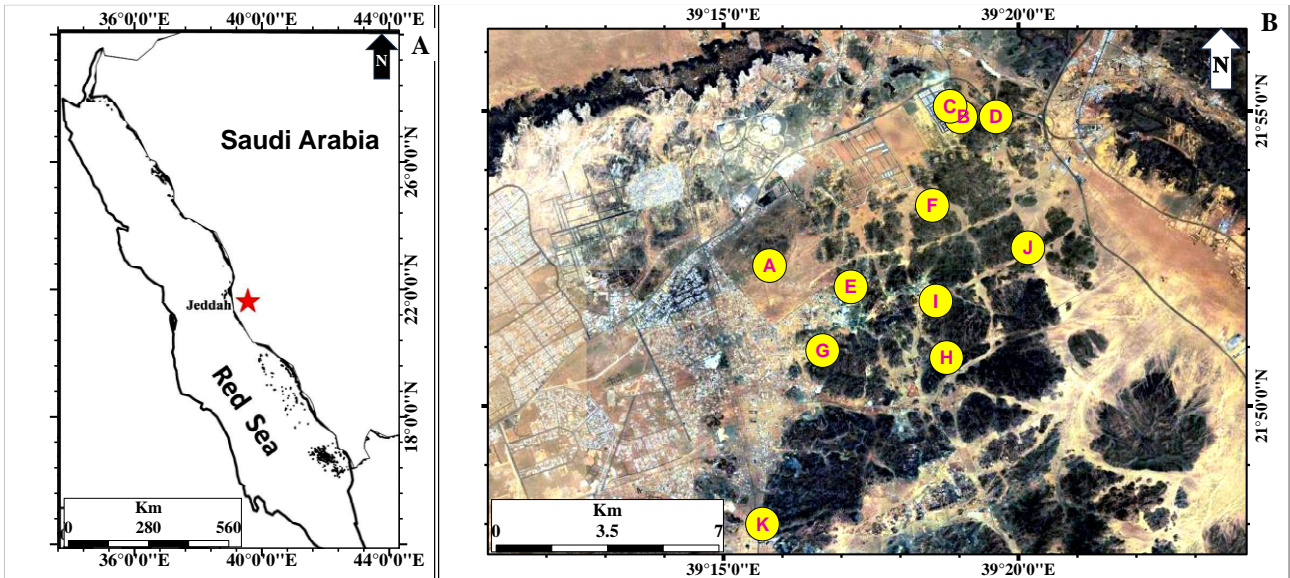


Fig. 1: Location map and a Landsat image showing the stations of the study area

### 3. Geological setting

The geology of the study area, which is a part of the Arabian Shield, includes Proterozoic crystalline basement rocks, tertiary sedimentary and volcanic rocks, and Quaternary deposits (Spencer et al., 1988). Mesaed et al. (2020) wrote that the basement rock is composed of igneous and metamorphic

geologic formations. Tertiary sedimentary rocks are mudstone, siltstone, and sandstone, whereas volcanic rocks (Harrat) are basalt and dolerite. Finally, quaternary wadi deposits include gravel, sand, silt, and clay. The average direction of the lineament is N15W which is evident from Fig. 2 (Alwash and Zakir, 1992).

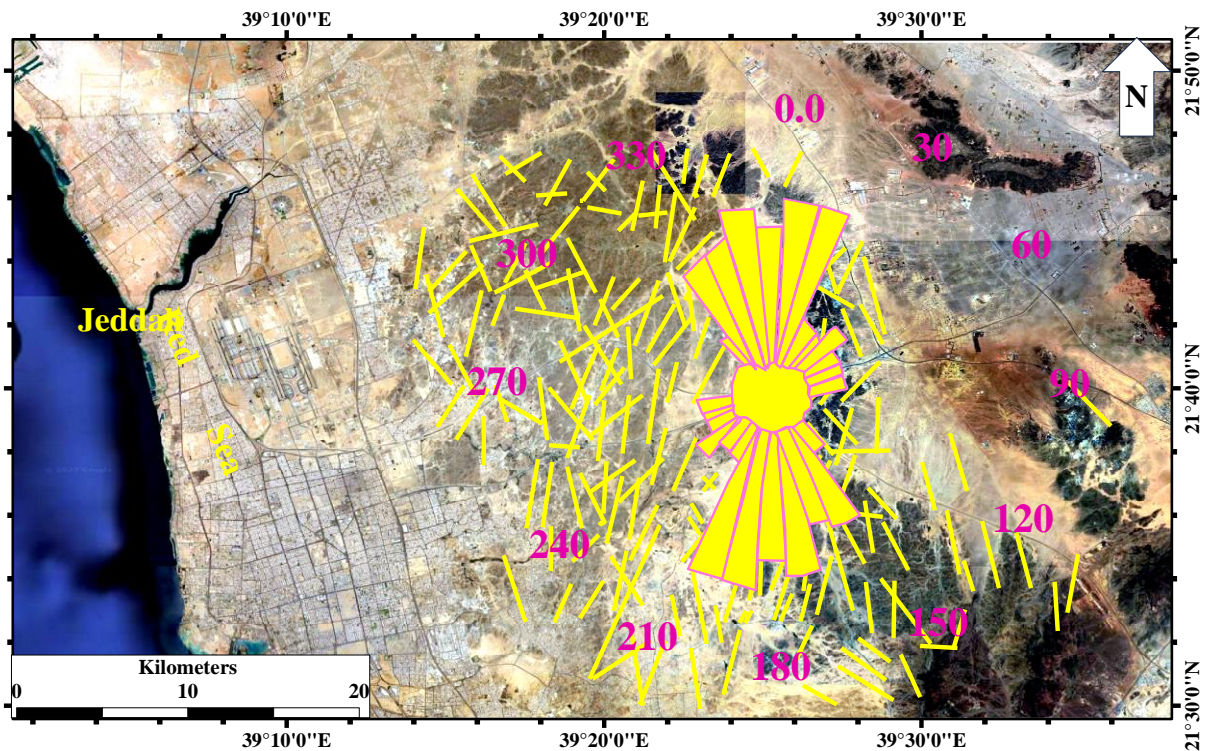


Fig. 2: Lineaments of the study area modified after (Alwash and Zakir, 1992)

### 4. Methodology

The Schmidt hammer field test is conducted approximately 3,000 times at 11 locations in the study area. Depending on the mathematical model,

UCS values are calculated, and a histogram of the recorded values is obtained. According to the skewness of the histogram, the Box and Whisker technique is used for the analysis. In addition, median, outliers and IQR values are used to evaluate

and compare the UCS issue in the study area. Finally, engineering geological maps are generated. Fig. 3 briefly shows the infographic of the methodological approach in this study. Application software such as

MS Excel and Arc GIS have been used for statistical analysis and engineering geological contour map drawing.

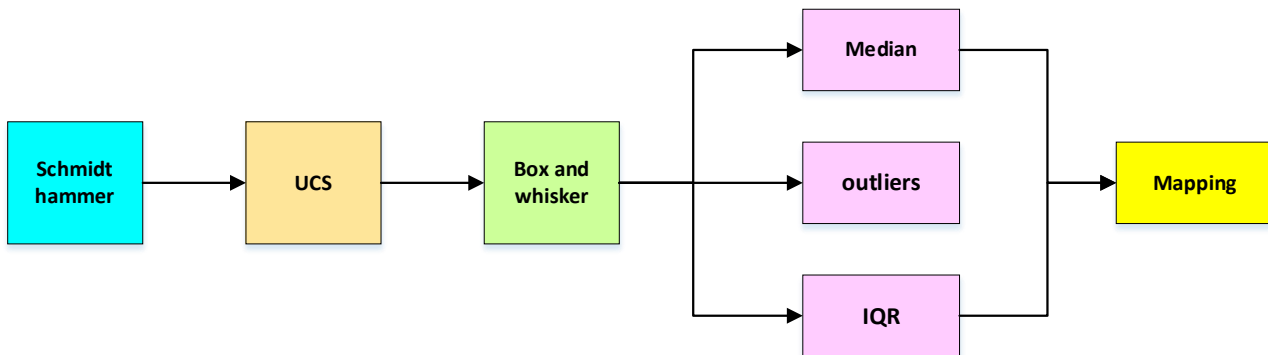


Fig. 3: Graphical approach of the research

In the common practice of rock engineering, the Schmidt hammer is widely used to indirectly estimate the rock's uniaxial compressive strength (Bolla and Paronuzzi, 2021). The standard methods for the Schmidt hammer test (ASTM, 2005) might be expected to ensure consistent and reliable values and reproducible correlations for a given rock type (Aydin and Basu, 2005). The Schmidt hammer test is used to obtain an approximate estimation of the uniaxial compressive strength of rock discontinuities (González de Vallejo and Ferrer, 2011). The L-type sclerometer consists of a cylindrical metal device containing a spring that drives a rod (and its hammer) out of the cylinder. Its rebound is measured when the hammer strikes the rock surface. The instrument is positioned perpendicular to a clean and free-from-cracks plane, and then the pressure is applied to the hammer until the spring is released. The spring rebound value is indicated on a scale on the side of the apparatus. The average value of five hammer blows is taken at each measuring point.

Empirical equations are developed to indirectly estimate UCS using physical properties such as Schmidt hardness number (Aladejare et al., 2021). Finally, the resulting rebound values are correlated with the uniaxial compressive strength using the following empirical formula (Wang and Wan, 2019).

$$UCS = \frac{6222}{88.15 - H_r} - 70.38$$

where,  $H_r$  is the Schmidt hammer rebound value,  $10 \leq H_r \leq 70$ .

The data collected for any geological engineering study of the properties and geotechnical characteristics of rock materials and masses should be statistically representative (González de Vallejo and Ferrer, 2011). Generally, the IQR with a measure of central tendency, such as the median, is used to understand the data's center and spread. According to the median and interquartile range (IQR), the Box and Whisker plotting technique (Acharya and Chellappan, 2017) is used to visualize the UCS data.

The IQR and median are used because they are robust variability and central tendency measures. Outliers dramatically influence none of the two measures because they are not dependent on each value. Compared to other ranges, extreme values, and outliers affect IQR less when measuring variability; furthermore, the median is an excellent representation of skewed distributions.

## 5. Results

Around 600 of UCS values at 11 locations, each reading is an average of five, are plotted in Fig. 4 and contoured in Figs. 5, 6, and 7. Over the entire study area, fluctuations in the UCS in different directions are also observed. For better evaluation and analysis of UCS, the descriptive statistic of each location is presented in Table 1 using MS Excel.

In order to evaluate the asymmetry of strength for the whole region, the histogram is introduced in Fig. 8. Based on the positive skewness observed in the histogram, the Box and Whisker method, as in Fig. 9, is used to evaluate the central and dispersion of UCS.

## 6. Discussion

The average UCS median for the whole area is 69 KPa, so the rock strength can be classified as strong (Brown, 1981) criterion. It is observed that sites B, C, and K, located at the opposite ends of the study area, have the weakest strength, and A, in NW, falls into the intermediate class. Conversely, all other sites have stronger strength values than others.

To simplify the classification of UCS distribution, a minimum (maximum) value of 23(72) of IQR may be clustered according to the regional dispersion and skewness into five categories from very low to very high. The high dispersion reflects low skewness, as shown in Table 2. With IQR values of 23 and 72, site K has the slightest variation and skewed strength distribution, while site B reflects the highest.

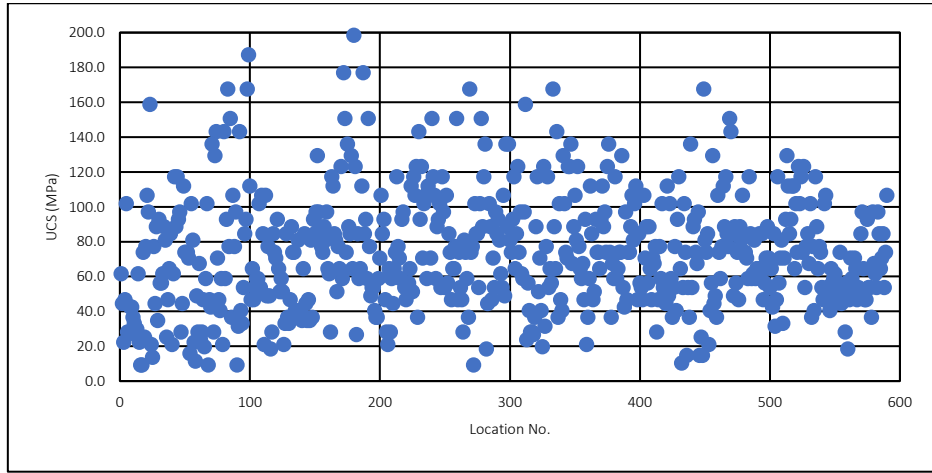


Fig. 4: Plotting of UCS

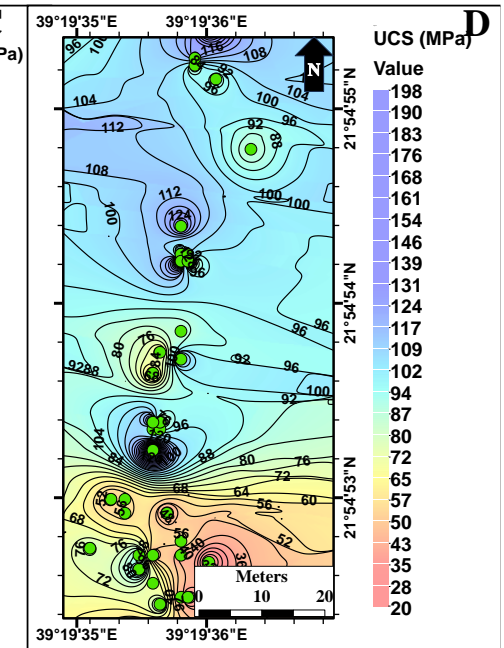
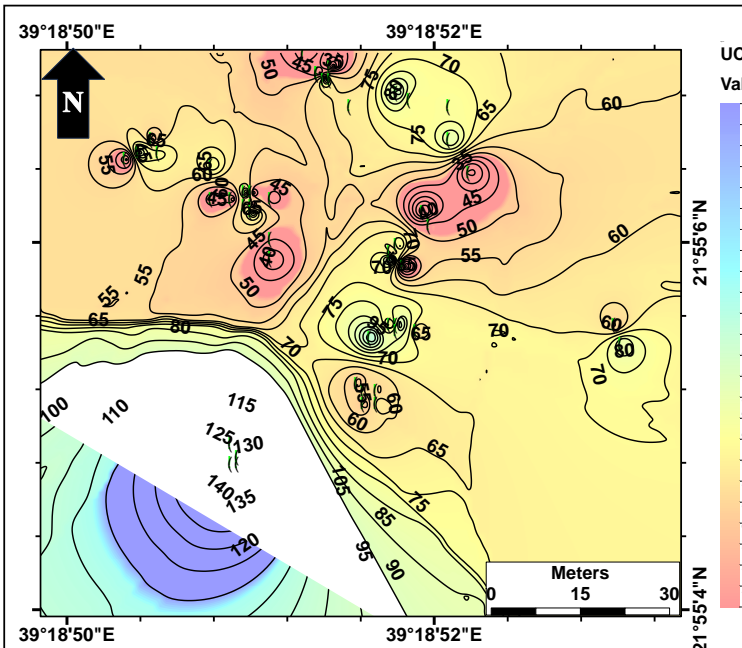
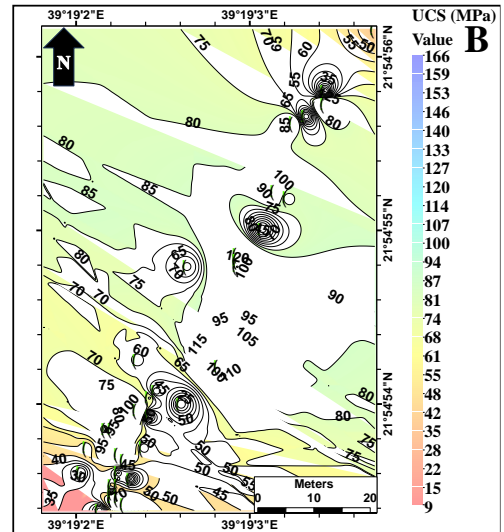
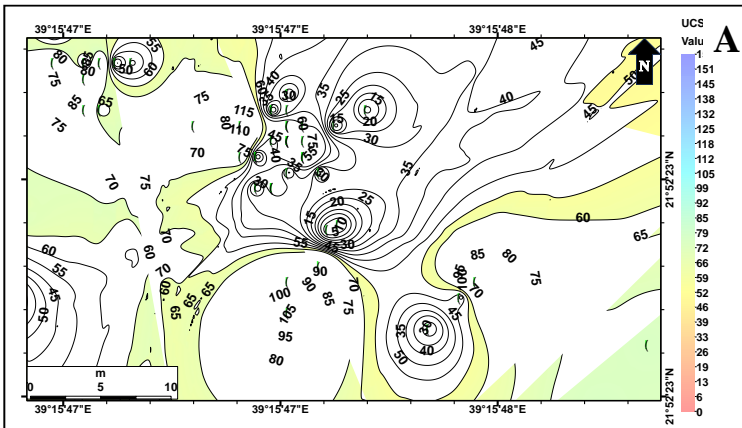


Fig. 5: Distribution of UCS at areas A, B, C, and D

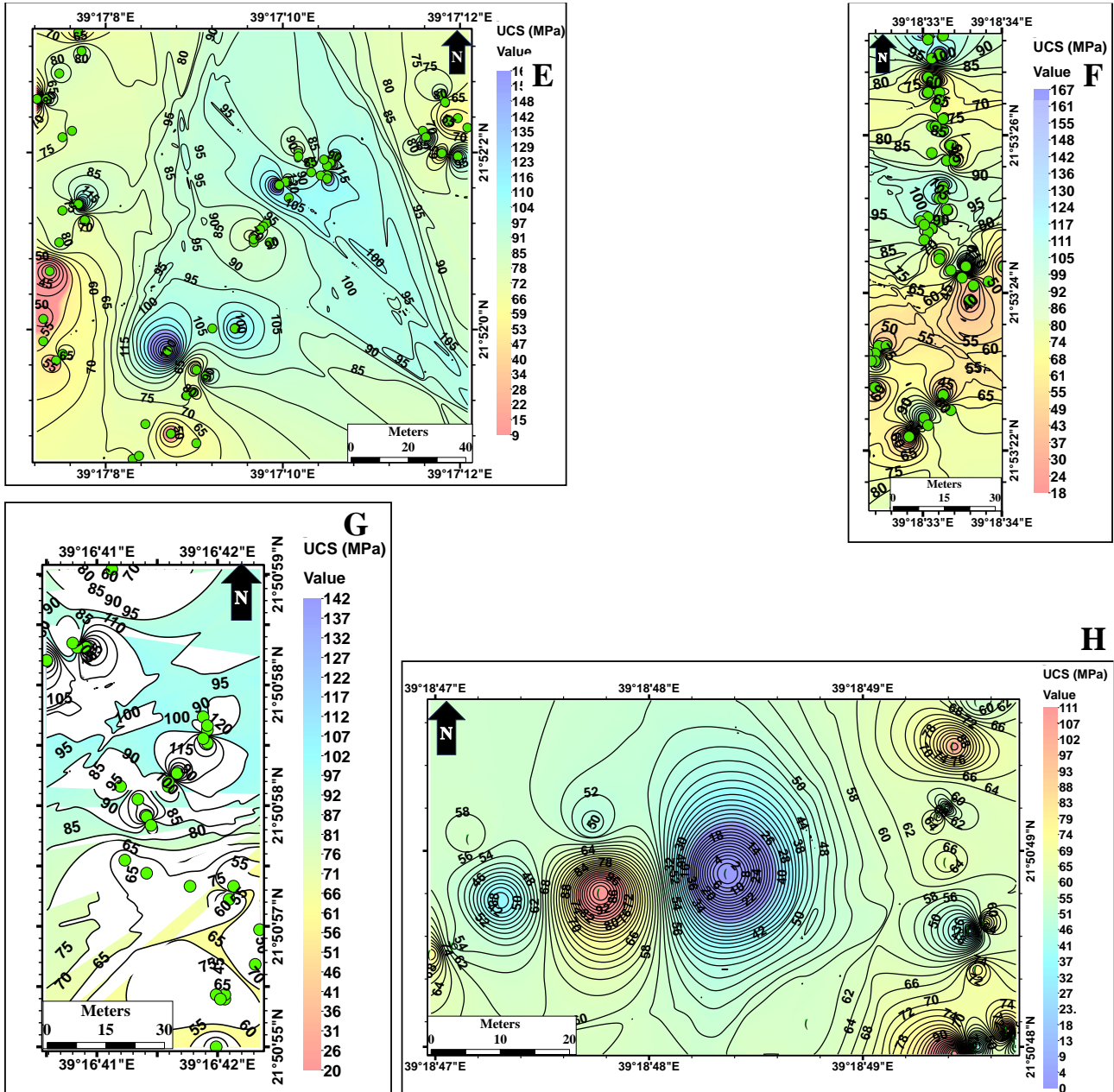


Fig. 6: Distribution of UCS at areas E, F, G, and H

Table 1: Descriptive statistics of UCS at different locations

Descriptive statistics	A	B	C	D	E	F	G	H	i	J	K
Count	53	40	51	73	59	59	30	62	71	45	47
Mean	60.3	66.5	64.6	80.4	81.7	79.0	80.4	74.8	73.8	80.1	60.7
Standard error	4.6	7.2	4.7	4.3	4.2	4.7	6.1	3.2	3.8	4.0	2.7
Median	61.6	53.9	58.8	77.2	77.2	77.2	75.5	73.8	73.8	77.2	56.2
Mode	61.6	28.1	84.6	84.6	53.7	88.5	46.7	73.8	84.6	101.7	53.7
Standard deviation	33.2	45.3	33.4	36.7	32.6	36.3	33.5	24.9	32.0	27.0	18.6
Sample variance	1099.0	2056.6	1113.7	1347.9	1063.6	1318.6	1124.8	619.9	1026.0	727.5	345.8
Kurtosis	0.0	-0.6	3.6	1.2	0.0	-0.4	-1.0	-0.4	0.6	-0.9	0.3
Skewness	0.5	0.7	1.5	1.0	0.4	0.4	0.2	0.5	0.4	0.0	0.6
Range	149.6	158.3	168.9	177.5	158.3	149.2	122.1	107.8	157.3	98.0	88.3
Minimum	9.2	9.2	18.3	20.9	9.2	18.3	20.9	28.1	10.3	31.4	18.3
Maximum	158.8	167.6	187.3	198.4	167.6	167.6	143.1	136.0	167.6	129.4	106.6
Sum	3193.5	2659.3	3296.1	5872.7	4821.3	4660.4	2410.9	4637.4	5240.1	3605.3	2853.4
Confidence level (95.0%)	9.1	14.5	9.4	8.6	8.5	9.5	12.5	6.3	7.6	8.1	5.5

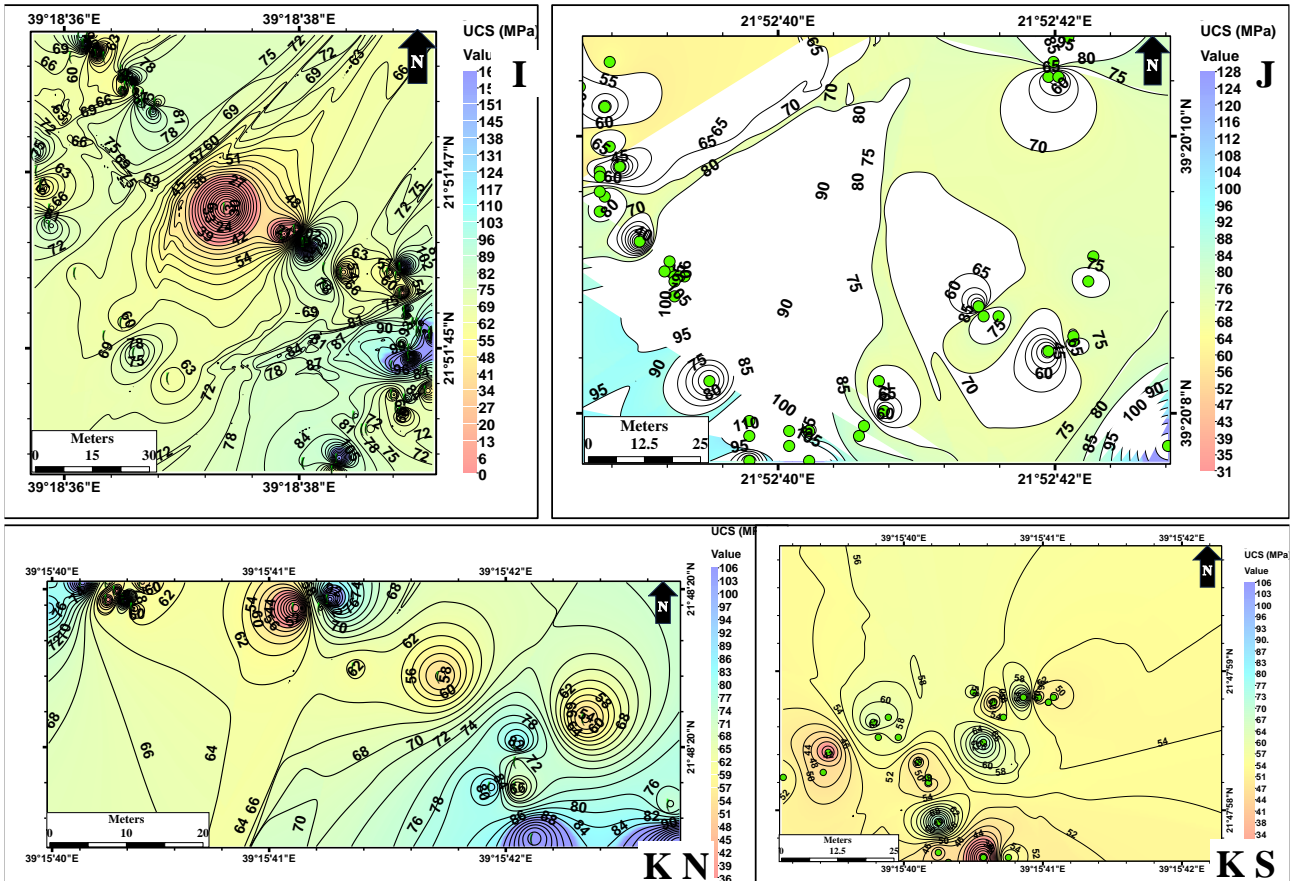


Fig. 7: Distribution of UCS at areas I, J, Kn, and Ks (Kn=K at north, Ks=K at south)

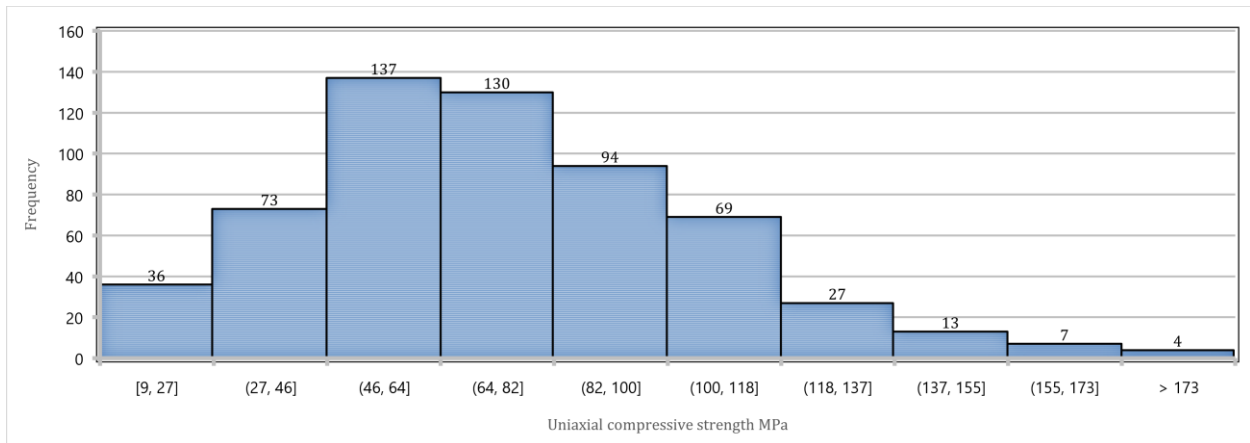


Fig. 8: Histogram of UCS of the whole sites

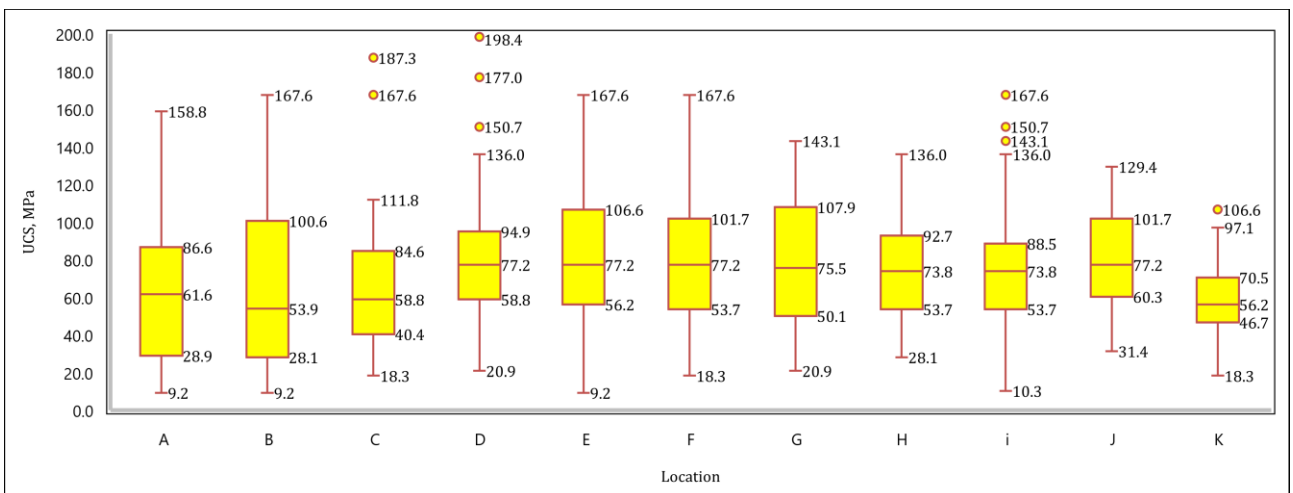


Fig. 9: Box and whisker of UCS for the whole investigated sites

**Table 2: Clustering of UCS dispersion**

Dispersion	Site	IQR
Very low	K	23
	I	34
Low	D	36
	H	39
	J	41
Medium	C	44
	F	48
	E	50
	G	57
High	A	57
	B	72

An engineering geological map (Fig. 10) is produced better to understand the UCS's median distribution throughout the region. While the results of the median of UCS show low values in the north, west, and southwest, they deliver high values in the core and east sides of the study area. Besides, the negative kurtosis value (wide dispersion) indicates that these changes may reflect the availability of multi-rock types, weathering, or heterogeneity.

The UCS variability is presented in Fig. 11 as a contouring map. It is possible to see that a high

dispersion of UCS appears in NE (location B), while the SW of the study area includes the least variability (location K). An increase in dispersion or variability may indicate the effect of other factors, such as specific rock type, mineralogy, or structure characteristics. Based on outliers (abnormal values located outside the whisker) in sites C, D, I, and K, as seen in Fig. 9, it is strongly recommended to investigate their availability reasons before eliminating them.

As one can understand from Table 1, based on the mean rather than the median, the average UCS for site A is the minimum (60.25 Mpa), while location E has the maximum (81.72 Mpa). Therefore, the confidence interval with a 95% confidence level for the entire area means for UCS at location A equals  $60.25 \pm 9.14$  MPa or 51.12 to 69.39 MPa. In contrast, location B ranges from  $81.72 \pm 8.50$  or 73.22 to 90.22 MPa. Fig. 12 shows the confidence interval at different locations of the study area. The changes in confidence interval may reflect the changes in lithology.

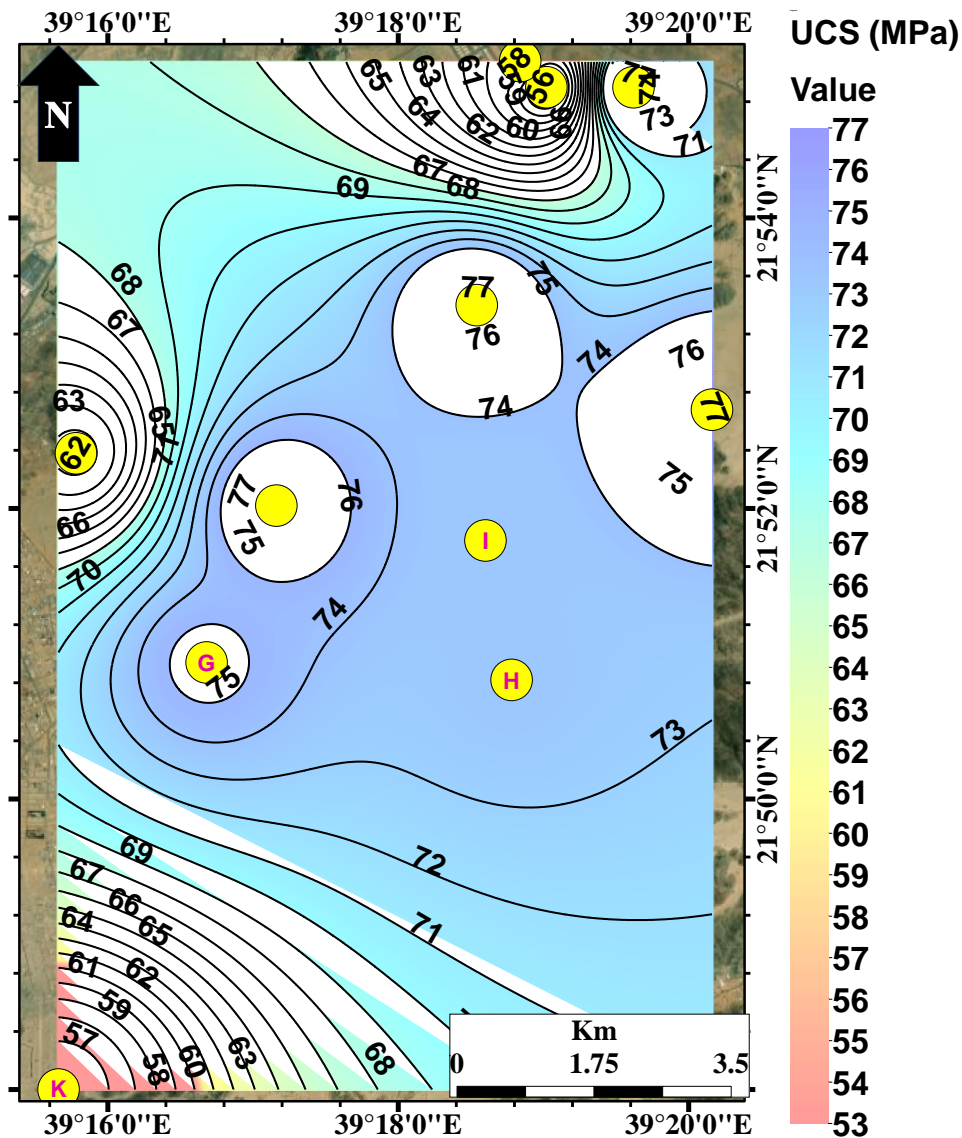


**Fig. 10: Median of UCS (Mpa)**

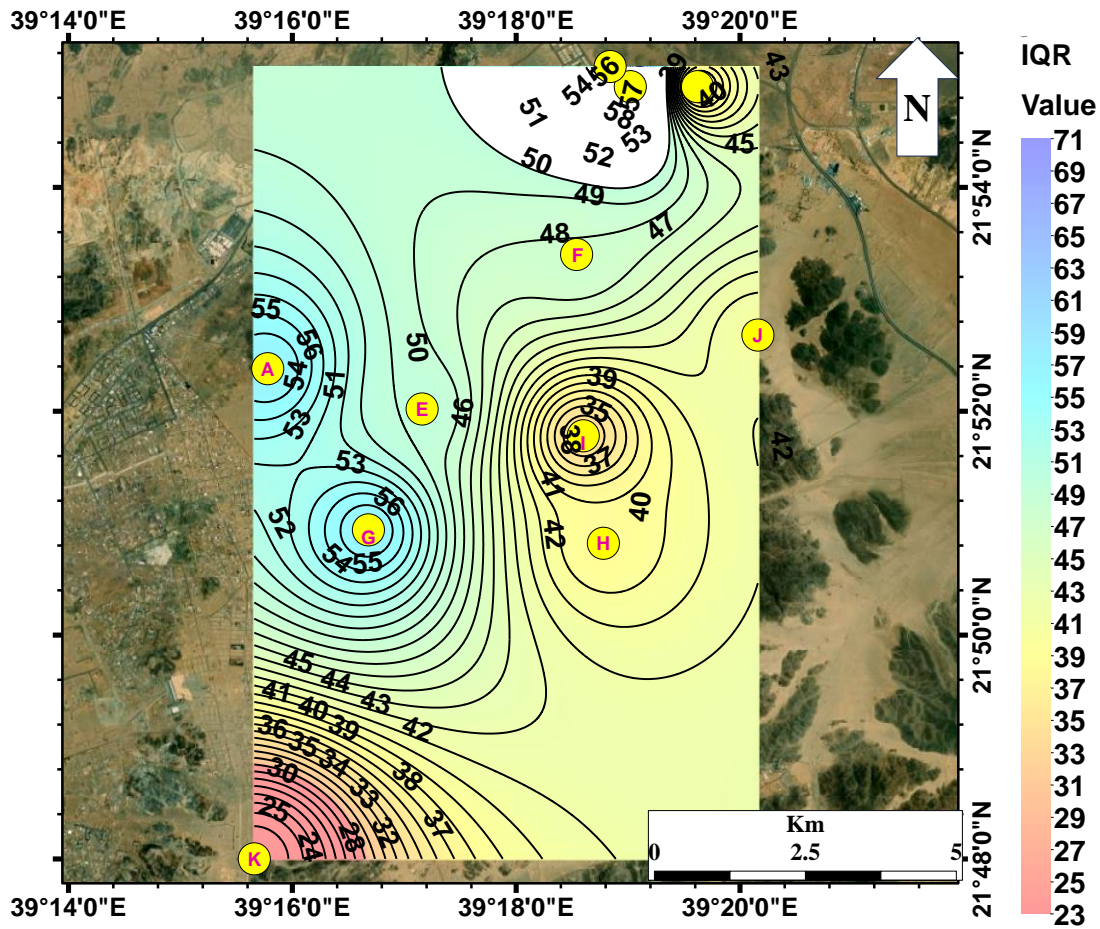


Fig. 11: IQR distribution

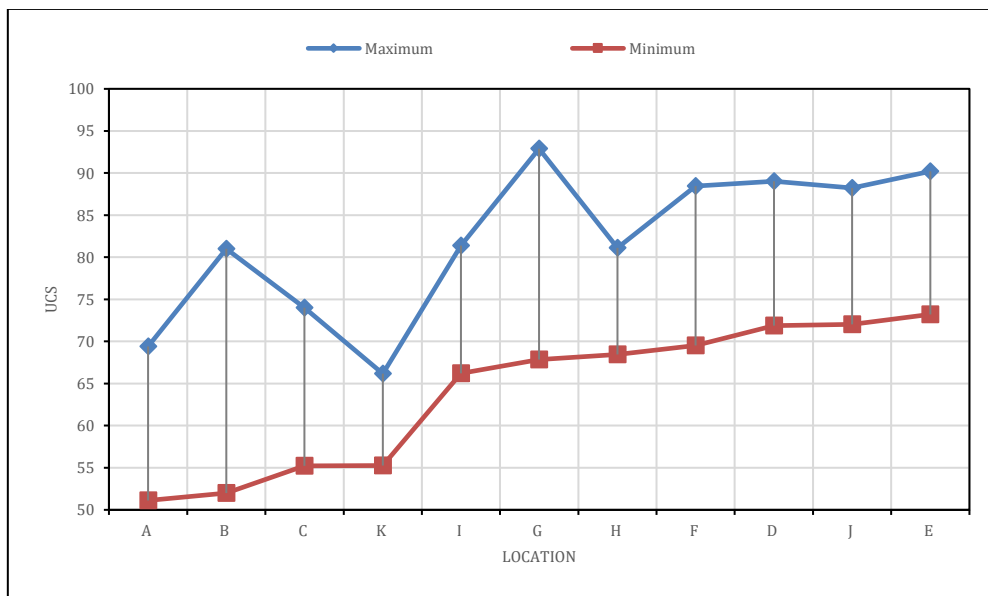


Fig. 12: Confidence interval of the mean of UCS

**7. Conclusion**

The assessment of the UCS of Proterozoic igneous rock formations in the northern region of Jeddah yields the subsequent findings:

1. The unconfined compressive strength exhibits a broad spectrum, ranging from 9 to 198 MPa.
2. When considering the standard deviation as a measure of dispersion, it is evident that the strength characteristics span from weak to exceptionally robust across the entire study area, with the exception of sites H and J, where the rocks fall within the range of moderate to very strong.
3. The frequency distribution of UCS, depicted in the form of a histogram, manifests a positively skewed distribution.



4. The median value of UCS for the entire study area is determined to be 69 KPa. Accordingly, in accordance with the guidelines established by the International Society for Rock Mechanics (ISRM), the rock strength classification can be denoted as 'strong.'

### Compliance with ethical standards

### Conflict of interest

The author(s) declared no potential conflicts of interest with respect to the research, authorship, and/or publication of this article.

### References

- Acharya S and Chellappan S (2017). Pro Tableau: A step-by-step guide. Apress, Berkeley, USA.  
<https://doi.org/10.1007/978-1-4842-2352-9>
- Aladejare AE, Alofe ED, Onifade M, Lawal AI, Ozoji TM, and Zhang ZX (2021). Empirical estimation of uniaxial compressive strength of rock: Database of simple, multiple, and artificial intelligence-based regressions. *Geotechnical and Geological Engineering*, 39: 4427-4455.  
<https://doi.org/10.1007/s10706-021-01772-5>
- Alwash MA and Zakir FAR (1992). Tectonic analysis of the Jeddah Taif area on the basis of LANDSAT satellite data. *Journal of African Earth Sciences (and the Middle East)*, 15(2): 293-301.  
[https://doi.org/10.1016/0899-5362\(92\)90076-0](https://doi.org/10.1016/0899-5362(92)90076-0)
- ASTM (2005). Standard test method for determination of rock hardness by Rebound hammer method. ASTM International, West Conshohocken, USA.
- Aydin A and Basu A (2005). The Schmidt hammer in rock material characterization. *Engineering Geology*, 81(1): 1-14.  
<https://doi.org/10.1016/j.enggeo.2005.06.006>
- Bewick RP, Amann F, Kaiser PK, and Martin CD (2015). Interpretation of UCS test results for engineering design. In the 13<sup>th</sup> ISRM International Congress of Rock Mechanics, OnePetro, Montreal, Canada.
- Bolla A and Paronuzzi P (2021). UCS field estimation of intact rock using the Schmidt hammer: A new empirical approach. In *IOP Conference Series: Earth and Environmental Science*, 833(1): 012014. <https://doi.org/10.1088/1755-1315/833/1/012014>
- Brown ET (1981). Rock characterization, testing and monitoring: ISRM suggested methods. Pergamon Press, Oxford, UK.
- González de Vallejo LI and Ferrer M (2011). Geological engineering. CRC Press/Balkema, Leiden, Netherlands.  
<https://doi.org/10.1201/b11745>
- Mesaed AA, Alghamdi MA, and Sonbul AR (2020). Landforms evolution of Wadi Qudaid area, west central Arabian shield, Saudi Arabia: An example of the role of the geological factors in the urban extensions. *Open Journal of Geology*, 10(6): 612-640. <https://doi.org/10.4236/ojg.2020.106028>
- Morita N (2021). Numerical methods for the borehole breakout problems using Geo3D. In: Morita N (Ed.), *Finite element programming in nonlinear geomechanics and transient flow*: 241-345. Gulf Professional Publishing, London, UK.  
<https://doi.org/10.1016/B978-0-323-91112-2.00017-3>  
**PMCID:PMC8616739**
- Spencer CH, Cartier A, and Vincent PL (1988). Industrial mineral resources map of Jiddah, Kingdom of Saudi Arabia. Ministry of Petroleum and Mineral Resources, Jeddah, Saudi Arabia.
- Wang M and Wan W (2019). A new empirical formula for evaluating uniaxial compressive strength using the Schmidt hammer test. *International Journal of Rock Mechanics and Mining Sciences*, 123: 104094.  
<https://doi.org/10.1016/j.ijrmms.2019.104094>
- Yılmaz I and Sındır H (2002). Correlation of Schmidt hardness with unconfined compressive strength and Young's modulus in gypsum from Sivas (Turkey). *Engineering Geology*, 66(3-4): 211-219. [https://doi.org/10.1016/S0013-7952\(02\)00041-8](https://doi.org/10.1016/S0013-7952(02)00041-8)